Available online at www.sciencedirect.com
ScienceDirect
Catalysis Today 129 (2007) 194–199
CATALYSIS TODAY
www.elsevier.com/locate/cattod

Photocatalytic properties of Bi_2MoO_6 nanoparticles prepared by an amorphous complex precursor

A. Martínez-de la Cruz *, S. Obregón Alfaro, E. López Cuéllar, U. Ortiz Méndez

División de Estudios de Posgrado, Facultad de Ingeniería Mecánica y Eléctrica, Universidad Autónoma de Nuevo León, Pedro de Alba s/n, Ciudad Universitaria, C.P. 66451, San Nicolás de los Garza, N.L., Mexico

Available online 11 September 2007

Abstract

Nanoparticles of Bi_2MoO_6 have been synthesized using an amorphous complex precursor. The evolution of the oxide was followed by TGA/DTA, XRD and TEM in order to investigate the formation process, crystal structure and morphology of synthesized samples. The effects of calcination temperature on the morphology, surface area and properties of Bi_2MoO_6 nanoparticles have been investigated in detail. The photocatalytic activity of Bi_2MoO_6 nanoparticles was evaluated by degradation of rhodamine B molecules in water under visible light irradiation. The photocatalyst evaluation criteria involved the photocatalytic properties of samples at different calcination temperatures. The kinetic degradation of rhodamine B followed a first order reaction with $k = 2.2 \times 10^{-2}$ min^{-1} and $t_{1/2} = 31.6$ min for the best material obtained.

Keywords: Bi_2MoO_6; Nanoparticles; Photocatalytic properties; Molybdates

1. Introduction

Throughout last decades, heterogeneous photocatalysis has been positioned as a promissory efficient technology to resolve environmental and energy problems. Since the discovery of photocatalytic activity of TiO_2 by UV irradiation [1], many works have been written describing novel methods to synthesized photocatalysts with special characteristics to achieve a high catalytic activity in red–ox reactions. The major applications investigated for this technology are the colour removal and dyes destruction, reduction of chemical oxygen demand (COD), mineralization of hazardous organics and purification and disinfection of water [2]. Within the overall category of dyestuffs rhodamine B dye (RhB), see Fig. 1, is famous for the stability as dye laser material. It has become a common organic pollutant, so the photodegradation of RhB is important to the purification of dye effluents to avoid damage in aquatic organisms [3].

Recently, some binary oxides with perovskite and related structures have shown photocatalytic activity under irradiation with visible light [4–6]. In this sense, oxides with Aurivillius structure type have received special attention. Some authors have reported Bi_2WO_6 as an interesting photocatalyst for water splitting and photodegradation of organic compounds under visible light irradiation [7,8]. Moreover photocatalytic activity for O_2 evolution has been observed in the analogous phase Bi_2MoO_6 [9,10]. Particularly, the binary system Bi_2O_3–MoO_3 have received special attention due the capacity of several oxides belonging the system to act as catalysts in the partial oxidation of olefins to produce unsaturated aldehydes, unsaturated nitrides or dienes [11]. Bi_2MoO_6 is the most studied compound within this family due to its interesting properties such as ion conductive, dielectric capacity, and luminescent and catalytic properties.

Frequently the solid-state reaction method employed to obtain the photocatalyst leads to materials with poor photocatalytic activity due to the small surface area developed. The so-called soft chemistry methods have shown to be efficient to prepare better catalysts than those synthesized by classical methods. In this sense, Kudo and Hijii [8] have reported the synthesis of Bi_2MoO_6 by hydrothermal synthesis, additionally the mechanosynthesis has been also employed for this purpose [12]. Recently Zhang et al. [13] have reported the formation of Bi_2WO_6 nanoparticles through a complex organic precursor. In the present work, the procedure described by Zhang has been followed in order to obtain the analogous oxide

* Corresponding author. Tel.: +52 81 83 29 40 20; fax: +52 81 83 32 09 04.
E-mail address: azmartin@ccr.dsi.uanl.mx (A. Martínez-de la Cruz).

0920-5861/$ – see front matter
doi:10.1016/j.cattod.2007.08.004

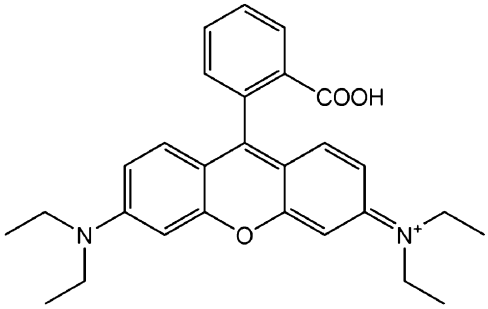

Fig. 1. Structure of Rhodamine B.

Bi_2MoO_6 with small particle size. The successful synthesis of nanoparticles of Bi_2MoO_6 will be providing an interesting candidate for photocatalytic applications.

2. Experimental

2.1. Preparation of samples Bi_2MoO_6

Bi_2MoO_6 was prepared via an amorphous complex precursor by means of a procedure that was described previously for the synthesis of Bi_2WO_6 [13]. The 0.034 mol of diethylenetriaminepentaacetic acid (H_5DTPA) (Aldrich, 99%) and 20 mL stronger ammonia water were put into 300 mL of hot distilled water. After dissolution, the 0.00984 mol Bi_2O_3 (Aldrich, 99.9%+) were added under a continuous stirring for 40 min in order to dissolve all the bismuth oxide. Then, 0.00143 mol $(NH_4)_6Mo_7O_{24}{\cdot}4H_2O$ (Productos Químicos Monterrey, 99%+) were added maintaining the solution with continuous stirring by another 40 min. It was stirred and heated at 80 °C in a water bath to promote the mixture. After the water was vaporized slowly, the solution became a piece of yellow transparent glass-like material. This material was used as precursor.

The precursor obtained was decomposed by thermal treatments at different calcination temperatures. Firstly, the material was heated at 200 °C by 1 h. After this initial thermal treatment, the powder was heated at 350, 375, 400, 450 and 900 °C (5 °C min^{-1}) by different periods of time in order to evaluate the formation of Bi_2MoO_6 from low temperatures. For comparative purposes, Bi_2MoO_6 was also synthesized by traditional solid-state reaction between Bi_2O_3 (Aldrich, 99.9%+) and MoO_3 (Merck, 99.9%+). A stoichiometric mixture was put into a porcelain crucible and then heated at 550 °C by 96 h to obtain the binary oxide.

2.2. Sample characterization

Structural characterization was carried out by powder X-ray diffraction using a Bruker D8 Advanced diffractometer with Cu Kα radiation doted with a Vantec high speed detector. X-ray diffraction data of bismuth molybdenum oxides were collected in the 2θ range of 10–70° with a scan rate of 0.05°/0.05 s. The morphology of the samples was analyzed by transmission electron microscopy. For this purpose a JEOL 2010 instrument with an accelerating voltage of 180 kV was used.

Thermogravimetric and differential thermal analyses (TGA/DTA) were performed on a TA Instruments Mod SDT Q600 thermal analyzer. The runs were carried out under a nitrogen atmosphere with a flux of 100 mL min^{-1} and with a heating rate of 5 °C/ min^{-1}. The surface area of the photocatalysts was determined by N_2 adsorption–desorption measurements by using a surface area and pore size analyzer Nova 2000e. The isotherms of adsorption–desorption were evaluated at −196 °C after a pretreatment of the sample at 100 °C during 2 h.

UV-diffuse reflectance spectrums of the oxides were measured by using a UV–vis spectrophotometer (Perkin-Elmer Lambda 35). The energy band gap (Eg) values for the different samples annealed were calculated using the equation $\alpha(h\nu) = A(h\nu - \mathrm{Eg})m/2$, where α is the absorption coefficient, $h\nu$ is the photon energy, A is a constant and $m = 2$ when represents a direct transition between valence band and conduction band. For the estimation of Eg from the UV–vis spectra, a straight line was extrapolated from the absorption curve to the abscissa axis. When α has a value of 0, then $\mathrm{Eg} = h\nu$.

2.3. Photocatalytic reactions

The photochemical reactor employed was a homemade device. The reactor have a glass borosilicate beaker surrounded with a water-jacket to maintain the reaction temperature at 25 ± 1 °C. A Xe lamp of 10,000 K with a luminous flux of 2100 lm was used as source of visible light. The photocatalytic activity of Bi_2MoO_6 was evaluated in the reaction of degradation of RhB in water. In a glass beaker, 220 mL of RhB solution (5 mg L^{-1}) containing 220 mg of photocatalyst were put in an ultrasonic bath to eliminate aggregates. The solution was reposed in dark conditions during 1 h to ensure the equilibrium adsorption–desorption of dye on the catalyst surface. After this time, the light source was turned on. During the reaction, samples of 8 mL were taken at given time intervals and then separated by centrifugation (4000 rpm, 20 min). The supernatant solution was decanted and the concentration of RhB was determined by the absorption band maximum (554 nm) using a UV–vis spectrophotometer (Perkin-Elmer Lambda 35).

3. Results and discussions

The material used as precursor of Bi_2MoO_6 was heated at 200 °C by 1 h in order to improve its handling. The resulting material was a red fine powder that was subsequently heated at 350, 375, 400, 450, 500 and 900 °C by different time intervals until to reach constant weight. To know the process formation of Bi_2MoO_6, TGA/DTA analyses were employed to follow the decomposition of precursor. Fig. 2 shows the TGA/DTA plot of the precursor powder at the temperature range 30–600 °C. Taking into account the amounts of starting materials, the theoretical weight loss must be 69.45% which is different of the experimental value of ∼57%. The difference observed between theoretical and experimental values can be due to the previous heating of the material at 200 °C for 1 h. Note that at this

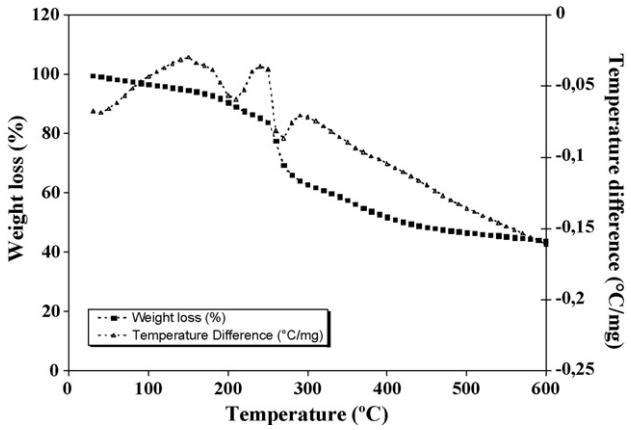

Fig. 2. TGA and DTA analysis of the precursor used to prepare Bi_2MoO_6 nanoparticles.

temperature, the TGA curve shows a weight loss near to 10%. Due to the involved stoichiometric amounts, it is very difficult to detect the process associated with the decomposition of $(NH_4)_6Mo_7O_{24}{\cdot}4H_2O$ (1.65% of total weight loss due to ammonium and water content). Until 200 °C, the continuous weight loss observed (∼10%) can be associated with water occluded in the material. The water associated with the decomposition of $(NH_4)_6Mo_7O_{24}{\cdot}4H_2O$ corresponds only to a 0.52%. The most important weight loss takes place from 200 to 400 °C. This event results from the decomposition of the different organic groups of the H_5DTPA. The weight loss of the sample takes place until 600 °C indicating that all organic material has been eliminated around this temperature. On the DTA curve, two endothermic peaks can be observed the first one around 210 °C and the second one at 270 °C, respectively. According with the knowledge about the decomposition process of the H_5DTPA, these peaks can be associated with the burning of hydrocarbon and amino-groups [13].

The X-ray diffraction results show good agreement with the TG/DTA analysis. Fig. 3 shows the X-ray diffraction patterns of decomposition species from the precursor at different calcination temperatures and for time expositions in which the weight loss was constant. The starting powder used as precursor undergoes important changes in colour with the increase of temperature, varying from the starting red colour to black, then brown, deep yellow, yellow and finally a pale-yellow colour at 200, 350, 375, 400, 450, 500 and 900 °C, respectively.

X-ray diffraction results show that below 350 °C, the material is amorphous. After the calcination temperature increases up to 350 °C, broad peaks of Bi_2MoO_6 (JCPDS Card no. 84-0787) appear with some impurities of Bi_2O_3 (JCPDS Card no. 65-1209). With the calcination temperature increase, the intensity of the diffraction lines of Bi_2MoO_6 increases and becomes sharper. On the other hand the impurity of Bi_2O_3 disappears. At 450 °C new diffraction lines that can be associated with the phase $Bi_{26}Mo_{10}O_{69}$ appear (JCPDS Card no. 89-0563). The intensity of these diffraction lines increase at 500 °C. Finally, the oxide Bi_2MoO_6 undergoes a crystalline transition to its high temperature polymorph (H-Bi_2MoO_6) when the calcination temperature increases to 900 °C. The inverse relationship

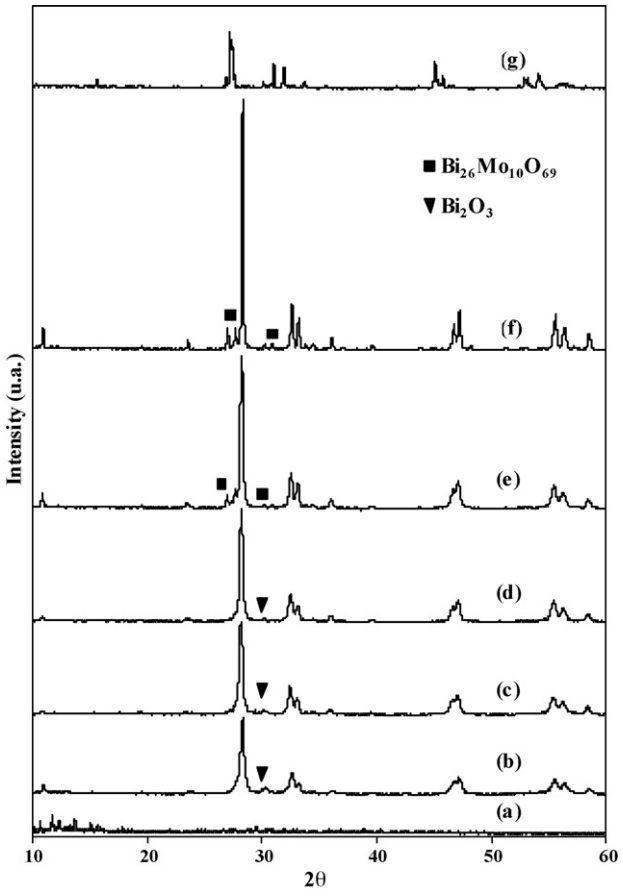

Fig. 3. XRD patterns of powders obtained under different calcination temperatures of the precursor: (a) 200 °C, (b) 350 °C, (c) 375 °C, (d) 400 °C, (e) 450 °C, (f) 500 °C and (g) 900 °C.

between the half-width of peak of the strongest line (Bi_2MoO_6) with the calcination temperature indicates a better crystallinity of the materials obtained at higher temperatures

The morphology of Bi_2MoO_6 was followed by TEM analysis. The samples analyzed were unstable to the electron beam due to decomposition of organic material remnant in each sample. To avoid this situation the samples were analyzed with low time exposition to the electron beam. Fig. 4 shows some TEM pictures of samples calcinated at different temperatures. A typical characteristic of the samples is the natural tendency to form aggregates. The lowest particle size detected in an isolated particle, around 30 nm, was observed in the sample obtained at 350 °C.

The particle size grew when calcination temperature was increased in the interval from 375 to 450 °C. Isolated particles from 50 to 100 nm, were observed. At 450 °C the particle size increased considerably reaching values around 200 nm.

The preparation of Bi_2MoO_6 nanoparticles can play an important role from the point of view of heterogeneous photocatalysis. As is well known, the critical step in the heterogeneous photocatalysis is the undesirable recombination of pair electron-hole before they reach the catalyst surface. In this sense, the small size of prepared particles reduces the pathway from the site of generation of the pair electron-hole to the catalyst surface.

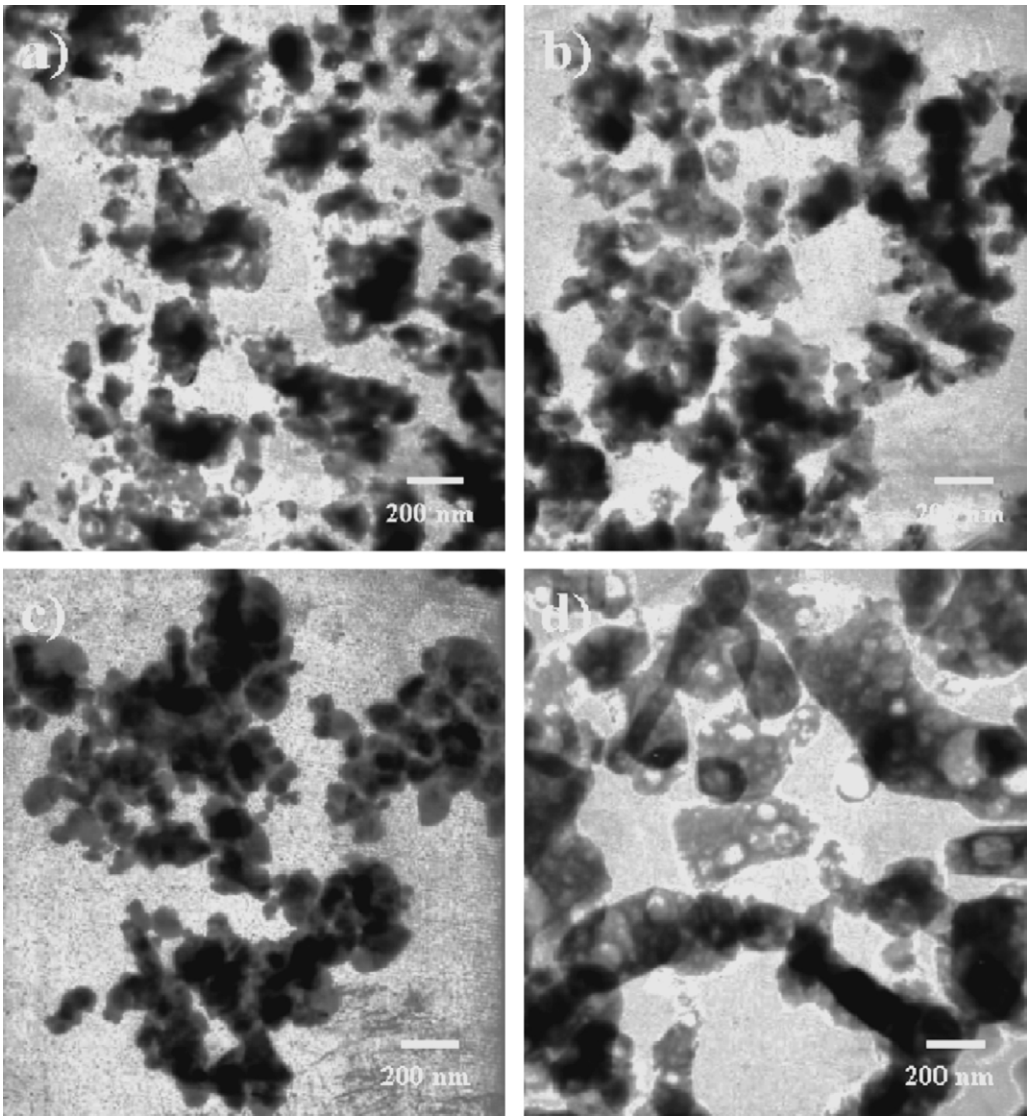

Fig. 4. Morphologies of temperature series Bi_2MoO_6 samples analyzed by TEM: (a) 350 °C, (b) 375 °C, (c) 400 °C and (d) 450 °C.

Table 1 shows another characteristic of the Bi_2MoO_6 nanoparticles. The relative low energies band gap obtained for Bi_2MoO_6 nanoparticles, <3.0 eV, leads to an important absorption of these materials in the visible spectrum. The band gap values obtained in the interval from 2.33 to 2.59 eV are lower than the obtained for the same oxide prepared by solid state reaction (2.64 eV) and by reflux method (2.7 eV) [9,10]. The differences observed in the values of Eg can be associated to the presence of residual organic material. The analysis by BET technique has revealed similar surface areas for the samples prepared by the amorphous complex precursor. These values are ten times higher than the obtained for a sample prepared by traditional solid state reaction (around 0.64 $m^2\ g^{-1}$) [7]. In order to estimate the crystal size behaviour of the samples as function of the calcination temperature, the half-width of the strongest line of Bi_2MoO_6 was followed. Taking these data the crystal size of the samples was calculated through Scherrer method [14]. As expected, the size of the

Table 1
The physical characteristics of Bi_2MoO_6 samples obtained at different calcination temperatures

Calcination temperature (°C)	Band gap (eV)	Surface area ($m^2\ g^{-1}$)	Half-width of the strongest line (deg)	Crystal size (nm)
350	2.33	7.37	0.3824	23.8
375	2.48	6.09	0.3441	26.5
400	2.51	7.90	0.3059	29.8
450	2.59	4.55	0.2422	37.6
500	2.53	6.73	0.1530	59.5

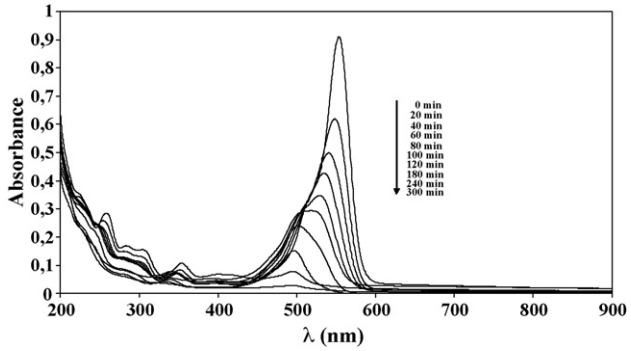

Fig. 5. Absorption changes of RhB solution under photocatalytic process (220 mg Bi_2MoO_6 prepared at 450 °C added into 220 mL of 5 mg L^{-1} RhB solution).

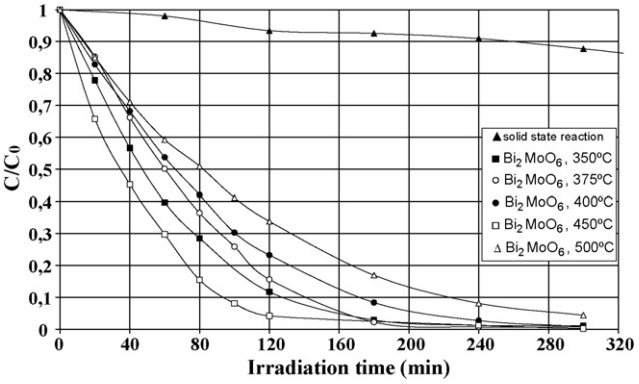

Fig. 6. Changes in RhB concentration during the course of photocatalytic degradation of RhB (5 mg L^{-1}) in the presence of Bi_2MoO_6 (1 g L^{-1}).

crystal increases with the increase of the calcination temperature. These values were ranged in the interval from 24 to 60 nm.

The photocatalytic activity of Bi_2MoO_6 nanoparticles was evaluated by degradation of rhodamine B in aqueous solution under visible light irradiation. The temporal evolution of spectral changes during the photodegradation process of RhB by Bi_2MoO_6 synthesized at 450 °C (the best photocatalyst) is displayed in Fig. 5.

The strong absorption band of RhB located at 554 nm is due the presence of four ethylated groups on the dye molecule, see Fig. 1. Visible light irradiation of the Bi_2MoO_6/RhB dispersion for 20 min produces a depleted in the original absorbance value of 33%. This result shows a high photocatalytic activity of Bi_2MoO_6 particles in the remove the chromosphere groups of RhB. The decrease in the absorption band of RhB was accompanied of a shift toward to blue region reaching a value around 500 nm after 2 h. The continuous colour change of the solution aqueous and the displacement observed in the strong absorption band can be justified as follows: according with previous works, the RhB photodegradation follows a mechanism that involves the formation of successive de-ethylated intermediates which respective maximum absorption bands are: *N*,*N*,*N*′-triethylated rhodamine, 539 nm; *N*,*N*′-diethylated rhodamine, 522 nm; *N*-ethylated rhodamine, 510 nm; and rhodamine, 498 nm [15]. Having in mind this data, it is possible to conclude that after 300 min at least, the four ethylated groups were removed of the organic dye.

Fig. 6 shows the temporal evolution of the RhB concentration when Bi_2MoO_6 with different calcination temperatures were employed. In general, all samples were able to degrade RhB but the sample prepared at 450 °C shows the higher photocatalytic activity. The kinetic data of Fig. 6 can be adjusted according with the first-order reaction equation, $\ln (C/C_o) = -kt$, where C_o and C are the concentrations of RhB before and after the irradiation (mg L^{-1}), t the time (min) and k is the apparent reaction rate constant (min^{-1}). For a RhB solution with an initial concentration of 5 mg L^{-1} containing 1 g L^{-1} of Bi_2MoO_6 obtained at 450 °C, the value of k is 2.2×10^{-2} min^{-1}. On the basis of this model, the half-life period of RhB, $t_{1/2}$, was found to be 31.6 min.

A notable difference on the photocatalytic activity was observed between the samples prepared by the amorphous complex precursor and the sample synthesized by solid-state reaction. In this sense, the sample obtained at 450 °C was over 50 times better photocatalyst than the sample synthesized by solid-state reaction. Undoubtedly, the route of synthesis by the amorphous complex precursor provides samples with high surface area and therefore an important photocatalytic activity. The variation of the efficiency of the photocatalysts studied in relation with the temperature of preparation is plotted in Fig. 7.

A decrease on the photocatalytic activity of the samples was observed as calcination temperature was increased in the interval from 350 to 400 °C. As is well known the surface area and cristallinity degree of the photocatalyst play a determinant role in the photocatalytic activity. Unfortunately these factors work in opposite directions, i.e. samples with a higher surface area can be obtained at lower temperatures but with a low crystallinity degree. The former effect leads to a high concentration of defects on the crystalline structure of the oxide. These defects work as recombination points of electron and holes formed during the excitation of the semiconductor oxide by light irradiation. In this sense, the factor that rules the photocatalytic activity of the Bi_2MoO_6 nanoparticles prepared at 350–400 °C is the surface area of the photocatalyst. For the 450 °C a notable increase on the photocatalytic activity was observed. At this temperature, extra X-ray diffraction peaks associated with the phase $Bi_{26}Mo_{10}O_{69}$ appears. The intensity

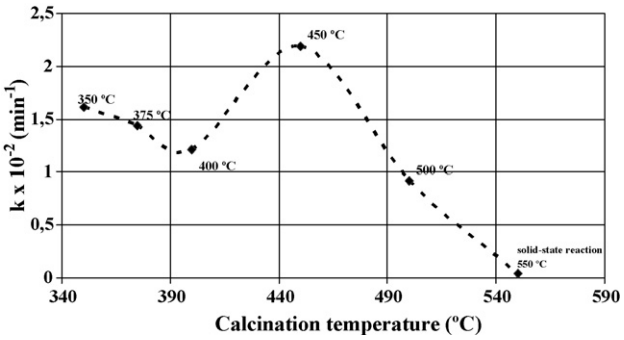

Fig. 7. Variation of the apparent reaction rate constant k (min^{-1}) for the photocatalytic degradation of RhB (C_o = 5 mg L^{-1}) using Bi_2MoO_6 calcinated at different temperatures.

of these peaks was higher at 500 °C showing that the concentration of $Bi_{26}Mo_{10}O_{69}$ crystalline was increased. Nevertheless, the photocatalytic activity of the sample decreases even more than on samples prepared at 350, 375 and 400 °C. This situation eliminates the possibility that $Bi_{26}Mo_{10}O_{69}$ plays an important role on the increase of the photocatalytic activity at 450 °C. Actually, the presence of $Bi_{26}Mo_{10}O_{69}$ has a negative effect on the efficiency of the materials. According with this observation it is possible to think that the crystallinity degree of material take a preponderant place on the photocatalytic process at 450 °C.

The photocatalytic degradation of RhB by Bi_2MoO_6 nanoparticles can be done by two ways. In first instance, by a true photocatalysis process where the irradiation over the photocatalyst promotes an electron from its valence band to the conduction band to form the pair electron-hole. The second possibility is through a process of photosensitization where the irradiation excited an electron from dye and then it is injected to the conduction band of the semiconductor oxide. In our case the photocatalytic degradation of RhB by Bi_2MoO_6 is through the photosensitization of dye organic by action of visible light irradiation as was observed previously with another semiconductor oxide [16]. This affirmation is formulated on the basis of experiments done using UV irradiation (254 nm and 365 nm) over Bi_2MoO_6/RhB dispersions. In the experiments carried out with both monochromatic irradiation, aqueous solution of RhB in presence of the photocatalyst Bi_2MoO_6 were stable after long time of UV irradiation.

4. Conclusions

Nanoparticles of Bi_2MoO_6 were prepared successfully by a method that involves an amorphous complex precursor. This route provides the possibility to obtain Bi_2MoO_6 until 200 °C below of the temperature employed by solid state reaction. This situation leads to the preparation of materials with higher surface area and small particle size. These factors contribute to consider to Bi_2MoO_6 as photocatalyst on reactions of dye-organic degradation with visible light irradiation. The photocatalytic activity of the materials was tested on the degradation of RhB. The relation between surface area and crystallinity degree produced a material with the higher photocatalytic activity at 450 °C. Taking into account that the degradation of RhB by Bi_2MoO_6 was performed through a mechanism of photosensitization of the dye-organic, the Eg value of semiconductor seems not to play an important role in the photodegradtion process.

Acknowledgements

We wish to thank to CONACYT for supporting the project 43800 and the Universidad Autónoma de Nuevo León (UANL) for its invaluable support through the project PAICYT-2006. We also thank Departamento de Ecomateriales y Energía of Facultad de Ingeniería Civil (UANL) for its assistance on the characterization of materials.

References

[1] K. Honda, A. Fujishima, Nature 238 (1972) 37.
[2] K. Kabra, R. Chaudhary, R.L. Sawhney, Ind. Eng. Chem. Res. 43 (2004) 7683.
[3] M. Asiltürk, F. Sayılkan, S. Erdemoglu, M. Akarsu, H. Sayılkan, M. Erdemoglu, E. Arpaç, J. Hazard. Mater. B 129 (2006) 164.
[4] A. Kudo, K. Omori, H. Kato, J. Am. Chem. Soc. 121 (1999) 11459.
[5] S. Kohtani, M. Koshiko, A. Kudo, K. Tokumura, Y. Ishigaki, A. Toriba, K. Hayakawa, R. Nakagaki, Appl. Catal. B 46 (2003) 573.
[6] C. Zhang, Y. Zhu, Chem. Mater. 17 (2005) 3537.
[7] J.W. Tang, Z.G. Zou, J.H. Ye, Catal. Lett. 92 (2004) 53.
[8] A. Kudo, S. Hijii, Chem. Lett. 28 (1999) 1103.
[9] J. Yuy, A. Kudo, Chem. Lett. 34 (2005) 1528.
[10] Y. Shimodaira, H. Kato, H. Kobayashi, A. Kudo, J. Phys. Chem. B 110 (2006) 17790.
[11] E. Vila, J.M. Rojo, J.E. Iglesias, A. Castro, Chem. Mater. 16 (2004) 1732.
[12] A. Castro, Bol. Soc. Esp. Ceram. Vidr. 41 (2002) 45.
[13] S. Zhang, C. Shang, Y. Man, Y. Zhu, J. Solid State Chem. 179 (2006) 62.
[14] B.D. Cullity, S.R. Stock, Elements of X-Ray Diffraction, Addison Wesley, 1978,, p. 102.
[15] T. Inoue, T. Watanabe, A. Fujishima, K. Honda, K. Kohayakawa, J. Electrochem. Soc. 124 (1977) 719.
[16] T. Watanabe, T. Takirawa, K. Honda, J. Phys. Chem. 81 (1977) 1845.